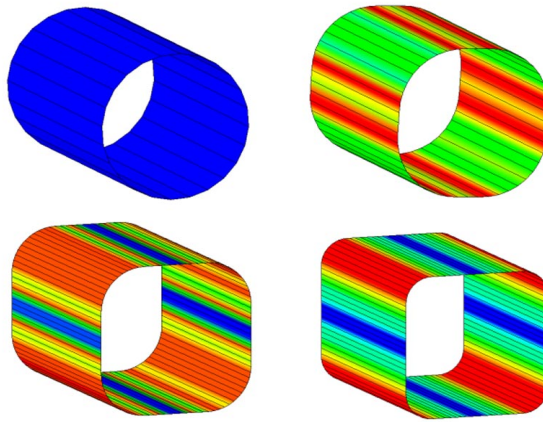




LUND
UNIVERSITY



A NEW H-ADAPTIVE METHOD FOR SHELL ELEMENTS IN LS-DYNA

IVAN OSKARSSON

Structural
Mechanics

Master's Dissertation

Div. of Structural Mechanics (LTH)

ISRN LUTVDG/TVSM--06/5141--SE (1-47)

ISSN 0281-6679

Dept. of Mechanical Engineering (IKP)

LITH-IKP-R -1408

A NEW H-ADAPTIVE METHOD FOR SHELL ELEMENTS IN LS-DYNA

Master's Dissertation by
Ivan Oskarsson

Supervisors:

Erik Serrano,
Div. of Structural Mechanics, LTH

Larsgunnar Nilsson,
Dept. of Mechanical Engineering (IKP), LiU

Copyright © 2006 by Structural Mechanics, LTH & Mechanical Engineering (IKP), LiU, Sweden.
Printed by KFS I Lund AB, Lund, Sweden, February, 2006.

For information, address:

Division of Structural Mechanics, LTH, Lund University, Box 118, SE-221 00 Lund, Sweden.
Homepage: <http://www.byggmek.lth.se>

Department of Mechanical Engineering (IKP), LiU, Linköping University, SE-581 83, Linköping, Sweden.
Homepage: <http://www.ikp.liu.se>

Preface

The work presented in this thesis was performed from September 2005 to February 2006 at the *Division of Solid Mechanics at LiTH* and the *Division of structural mechanics at Lund University*.

The idea to this thesis was formulated by *prof. Larsgunnar Nilsson* at Solid Mechanics.

First of all I would like to express my gratitude to my supervisor at LiTH, *prof. Larsgunnar Nilsson*. I also want to thank *PhD* student *Mikael Jansson* for helping me with the modelling and simulations in LS-DYNA.

Further, I would like to thank *Dr Erik Serrano* at the *Division of Structural Mechanics at LTH, Lund University*, for helping me with the outline of the thesis.

Linköping, February 2006

Ivan Oskarsson

Abstract

This thesis describes the development of a new h-adaptive method for shell elements in the explicit FE-code LS-DYNA. Adaptivity is used to obtain accurate results for large deformation analyses to a low computational effort. However, the present adaptive method available in LS-DYNA is based on a geometrical simplification. When the mesh is refined, the bending deformation of the shell is not considered. This simplification makes the strains and strain distribution improper in for example hydro-forming simulations with the adaptive method.

The new method is based on an improved description of the updated geometry. This is made by approximating the shape of the deformed structure and inserting new nodes on the approximated surface. Re-meshing is performed based on the new geometry and the simulation is restarted.

The method was applied in two hydro-forming simulations and results from the present adaptive method were compared to results from a reference analyses with a fixed mesh.

The conclusions of the new method for the analysed examples are:

- Improved accuracy in terms of strains compared to the present methods.
- Improved strain distribution compared to the other present adaptive methods.
- Probably more effective than the present two-pass method. That is improved accuracy in terms of strains to a lower computational effort.
- The method results in a loss of internal energy which leads to inaccurate stresses

Contents

1. Introduction.....	1
1.1 Background.....	1
1.2 Aim with thesis.....	1
1.3 Limitations.....	1
1.4 Method and tools.....	1
1.5 Outline of the thesis.....	2
2. Theory.....	3
2.1 Basic Structural dynamics.....	3
2.1.1 Governing equations.....	3
2.1.2 Structural damping.....	4
2.2 Central difference method.....	7
2.3 Shell elements.....	8
2.4 Principle of virtual work.....	9
2.5 Adaptive method.....	10
2.6 LS-DYNA.....	12
2.6.1 Explicit time integration.....	12
2.6.2 Belytschko-Lin-Tsay shell.....	14
2.6.3 Damping in LS-DYNA.....	15
2.6.4 Contacts.....	15
2.6.5 Control volume.....	16
2.6.6 H-adaptivity in LS-DYNA.....	18
3. Proposed method.....	21
3.1 Present adaptive method.....	21
3.2 About the proposed adaptive method.....	21
3.3 Approximating shape in 2 dimensions.....	23
4. Introductory examples.....	25
4.1 Linear elastic beam.....	25
4.2 Shell strip.....	26
5. Hydro-forming analyses.....	29
5.1 Expanding tube.....	29
5.1.1 Analyses.....	30
5.1.2 Results.....	32
5.2 Hydro-forming of a tube.....	32
5.2.1 Analyses.....	33
5.2.2 Results.....	34
6. Discussion of results.....	37
6.1 Discussion of the hydro-forming examples.....	37
6.2 Future development of the method.....	38
7. Conclusions.....	39
Appendix A.....	43
Appendix B.....	45

1. Introduction

1.1 Background

In large deformation FE-analyses, such as crash worthiness and metal-forming applications, a fine element mesh is required to obtain accurate results. However, the computational effort increases with an increasing number of elements in the model. In the FE-code LS-DYNA, an h-adaptive method is frequently used. A problem with this method is that the refinement process does not consider the deflection of the elements, since displacements are only evaluated at the element nodes. This may lead to inaccurate results concerning strain and strain distribution.

1.2 Aim with thesis

The primary aim of this thesis is to investigate and develop a new technique for the h-adaptive method for shell elements in LS-DYNA. The purpose with the new method is to obtain a more accurate solution in terms of strain and strain distribution. The new technique will be compared to the present method and with a reference solution in different analyses. The main task is thus to distinguish differences in the results. Also the required CPU-time for the analyses is of great interest, since one of the objectives of the adaptive method is to decrease the total computational time. Possible losses in total energy with the new method will also be discussed.

1.3 Limitations

This thesis is performed during 20 weeks, which makes its context somewhat limited. The new method is therefore limited to 2-dimensional problems for shell elements. The same theory is valid also in the 3-dimensional case, although this requires more effort. The 2-dimensional case is an appropriate approach to distinguish the differences between the present and the new h-adaptive method. The new method is only a development of one of the two different options for the adaptive solution methodology, the one-pass method. How the new method will affect the total energy of a simulation will not be taken into consideration but it will be noticed and discussed.

1.4 Method and tools

The basis of the new method is to improve the geometry description when the mesh is refined. This is made by approximating the shape of the deformed structure and also taking into account the bending deformation of the element. The procedure for the intended methodology can be divided into the following steps:

- Define initial mesh and start the analysis
- Stop analysis at a certain state
- Identify nodal displacements

- Approximate the true shape of the deformed structure
- Insert new nodes and re-mesh
- Map the state variables from the previous solution
- Restart the analysis

The new solution methodology will be made manually and no implementation in LS-DYNA will be performed.

The analysis is made in LS-DYNA version 970 and the result is viewed in LS-Pre-Post, a postprocessor for LS-DYNA. To generate the shape and the new nodal coordinates a function in MATLAB has been written. The function has to be manually provided with input.

1.5 Outline of the thesis

The first part of Chapter 2 contains necessary theory to understand the methods used in LS-DYNA. Some basic structural dynamics, numerical methods, shell elements and general adaptive methods are described briefly. The second part discusses LS-DYNA and how the theory is implemented in the program.

In Chapter 3, the present adaptive method and its properties are treated. The initial problems with the present method are also discussed. The methodology for the new adaptive method is introduced.

Two introductory examples are presented in Chapter 4. The first example is a simple linear elastic beam model and the second is an elastic plastic shell strip, both exposed to a uniform pressure. The second example is evaluated to see if the proposed method is accurate enough.

In Chapter 5, more complex hydro-forming simulations are made. The new method will be compared to a reference solution and to the present adaptive method. The results of these two simulations will be a measure of how accurate the new method is in practice.

Chapter 6 contains a discussion of the results of, in particular, the hydro-forming simulations. Also, some opinions on future development and ideas how the software can be improved are presented.

In the last chapter, the final conclusions of the new method are stated.

2. Theory

To understand the context in this report one needs some basic theory about the methods used in LS-DYNA and how the program works. In the first part of this Chapter, basic theory about structural dynamics, shell elements, time integration and general adaptive methods will be discussed. In the second part, LS-DYNA is described.

2.1 Basic Structural dynamics

LS-DYNA is a FEM-program mainly for analysing large deformation dynamic response of structures. How dynamic problems are described mathematically and which methods that are used to solve the governing equations will be treated in the following chapters.

2.1.1 Governing equations

Consider a statically analysed structure. The equations of equilibrium for a linear problem require that:

$$f_{int} = f_{ext} \Leftrightarrow ku = f \quad (2.1)$$

That is, internal forces are equal to external forces. k denotes the linear stiffness of the structure and u the displacement

In a static non-linear analysis the internal force varies as a nonlinear function of displacements according to;

$$f_{int}(u) = f_{ext} \quad (2.2)$$

Now, consider the damped dynamic single degree of freedom, SDOF, system in Figure 2.1.

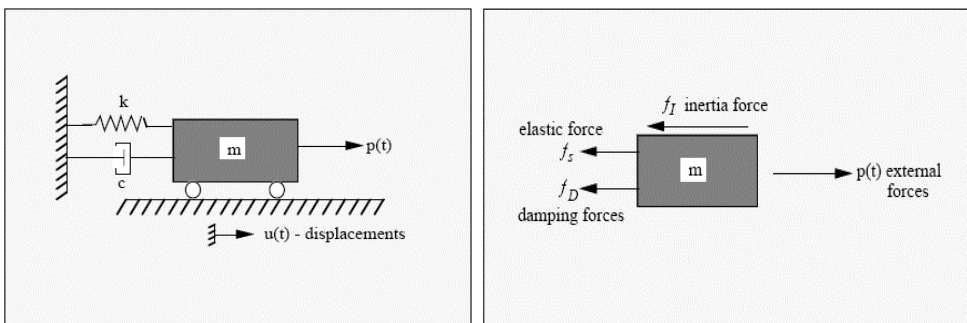


Figure 2.1: Single degree of freedom system [4]

Dynamic equilibrium requires that (d'Alembert's principle):

$$f_I + f_D + f_{\text{int}} = p(t) \quad (2.3)$$

Where:

$$f_I = m\ddot{u}; \quad \ddot{u} = \frac{d^2u}{dt^2}; \quad \ddot{u} = \text{acceleration} \quad (2.4-2.5)$$

$$f_D = c\dot{u}; \quad \dot{u} = \frac{du}{dt}; \quad \dot{u} = \text{velocity} \quad (2.6-2.7)$$

$$f_{\text{int}} = ku; \quad u; \quad u = \text{displacement} \quad (2.8-2.9)$$

k is as in static analysis the linear stiffness, c is the damping coefficient and m is the mass of the body.

Inserting Equations 2.4-2.9 in 2.3 leads to the *equation of motion*. In the linear case the equation of motion appears as a linear ordinary differential equation (o.d.e).

$$m\ddot{u} + c\dot{u} + ku = p(t) \quad (2.10)$$

In the nonlinear case, the internal force varies in the same manner as in the static nonlinear case. Therefore, the equation of motion appears as a non-linear o.d.e.

$$m\ddot{u} + c\dot{u} + f_{\text{int}}(u) = p(t) \quad (2.11)$$

For the linear o.d.e, analytical solutions are accessible but in the non-linear case only numerical solution methods are possible. [4]

2.1.2 Structural damping

In structural dynamic analyses the applied force is a function of time. If a typical load curve is used as in Figure 2.2 the response for a certain node in an undamped structure, $c = 0$, will appear as shown in Figure 2.3.

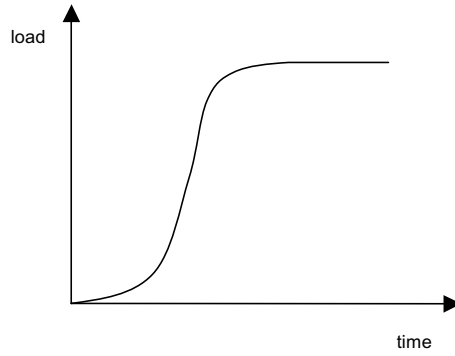


Figure 2.2: Typical load curve

That is, the structure will start to vibrate with a certain frequency, the natural angular frequency, ω_n . To obtain the static solution to the problem, structural damping has to be included. Some theory about structural damping and how the damping can be applied in a dynamic structure follows.

Consider the equation of motion, Equation 2.10, for an SDOF system. Now, with the modification that the vibration is said to be free. That is, the structure has been exposed to a displacement, $u(0)$, and thereafter been released. There is no exciting force acting on the structure.

$$m\ddot{u} + c\dot{u} + ku = 0 \quad (2.12)$$

c is, as described, earlier the damping coefficient. It describes the energy loss in a cycle of free vibration.

The natural frequency is calculated as:

$$\omega_n = \sqrt{\frac{k}{m}} \quad (2.13)$$

A new term called the damping ratio, ζ , is introduced. The relation between c and ζ is as follows:

$$\zeta = \frac{c}{2m\omega_n} \quad (2.14)$$

Dividing Equation 2.12 by m gives:

$$\ddot{u} + 2\zeta\omega_n\dot{u} + \omega_n^2u = 0 \quad (2.15)$$

The solution to this differential equation has the form:

$$u = e^{st} \rightarrow (s^2 + 2\zeta\omega_n s + \omega_n^2)e^{st} = 0 \quad (2.16)$$

This equation is satisfied for all t if:

$$s^2 + 2\zeta\omega_n s + \omega_n^2 = 0 \quad (2.17)$$

Equation 2.17, known as the *characteristic equation*, has two roots:

$$s_{1,2} = \omega_n(-\zeta \pm i\sqrt{1-\zeta^2}) \quad (2.18)$$

In the case when $\zeta = \pm 1$, the imaginary part will be zero. The solution to $s_{1,2}$ is exactly the undamped natural angular frequency. This case is called the critical damping of a system and c_{cr} is called the *critical damping coefficient* and can be expressed as:

$$c_{cr} = 2m\omega_n = 2\sqrt{km} = \frac{2k}{\omega_n} \quad (2.19)$$

Other types of damping that can occur in a dynamic system are underdamped and overdamped. The differences between undamped, underdamped and critical damping are shown in Figure 2.3.

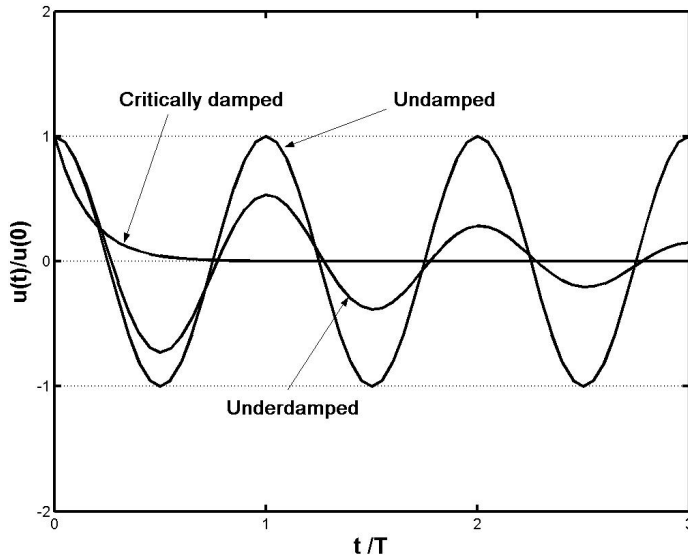


Figure 2.3: Dynamic response for different types of damping (adopted from [1])

On the y -axis, one has the ratio between the response at time t , $u(t)$, and the initial displacement, $u(0)$, and on the x -axis the ratio between the time t and the natural period time of the system, T_n , which is defined as:

$$T_n = \frac{2\pi}{\omega_n} \quad (2.20)$$

The above theory is described for one-dimensional single degree of freedom problems, scalar problems. In multi degree of freedom, MDOF , the same theory applies, with parameters described as matrices and vectors. That is, an MDOF-system has a set of different natural angular frequencies. Every frequency is said to describe a mode, that is a special vibration shape of the structure. For every mode there is a corresponding c_{cr} and therefore a corresponding response.

There are different methods of applying damping to a structure. Unlike the elastic modulus of a material, the properties of damping are not that well established. In classical damping theory there are different ways to express the damping coefficient c . One usually utilizes two main techniques, either mass-proportional damping or stiffness-proportional damping. A mix of these two makes the so called Rayleigh damping. Since the damping coefficient, as described earlier, varies in different modes it is a complex procedure to express the damping for a structure. Normally in structural dynamics, only the lowest modes (frequencies) are of interest for the response. [1]

2.2 Central difference method

As mentioned earlier only numerical solutions are available for the non-linear o.d.e. LS-DYNA uses the *central difference method*, c.d.m, to solve the equation of motion. C.d.m is an explicit time scheme since the unknown state variables only are functions of known variables as shown below. [4] Difference methods are appropriate for approximating derivatives of smooth curves.

$$U_{n+1} = f(U_n, U_{n-1}, \dots, t_{n+1}, t_n, t_{n-1}, \dots) \quad (2.21)$$

In this case, consider the smooth displacement function $u(t)$. Now, one wants to approximate the first and second derivatives, $\dot{u}(t)$ and $\ddot{u}(t)$, at a certain time t . Consider the Taylor expansion series for a given time step Δt .

$$u(t + \Delta t) = u(t) + \dot{u}(t)\Delta t + \frac{\ddot{u}(t)}{2}(\Delta t)^2 + \frac{\dddot{u}(t)}{6}(\Delta t)^3 + \dots \quad (2.22)$$

$$u(t - \Delta t) = u(t) - \dot{u}(t)\Delta t + \frac{\ddot{u}(t)}{2}(\Delta t)^2 - \frac{\dddot{u}(t)}{6}(\Delta t)^3 + \dots \quad (2.23)$$

Subtracting Equation 2.23 from 2.22 gives the central difference formula for the first derivative. When Δt is small this can approximately be written as:

$$\dot{u}(t) \approx \frac{u(t + \Delta t) - u(t - \Delta t)}{2\Delta t} \quad (2.24)$$

By adding 2.22 and 2.23, the second derivative can be approximated. This gives:

$$\ddot{u}(t) \approx \frac{u(t + \Delta t) - 2u(t) + u(t - \Delta t)}{(\Delta t)^2} \quad (2.25)$$

Let n denote the time step counter. A more compact way of expressing these equations can be written as [4]:

$$\dot{u}_n = \frac{1}{2\Delta t}(u_{n+1} - u_{n-1}) \quad (2.26)$$

$$\ddot{u}_n = \frac{1}{(\Delta t)^2}(u_{n+1} - 2u_n + u_{n-1}) \quad (2.27)$$

The central difference algorithm is illustrated in Figure 2.4.[5] The central difference method is however only conditionally stable and therefore the time steps need to be small.[4] How the size of the critical time step can be approximated will be treated in Chapter 2.6.1.

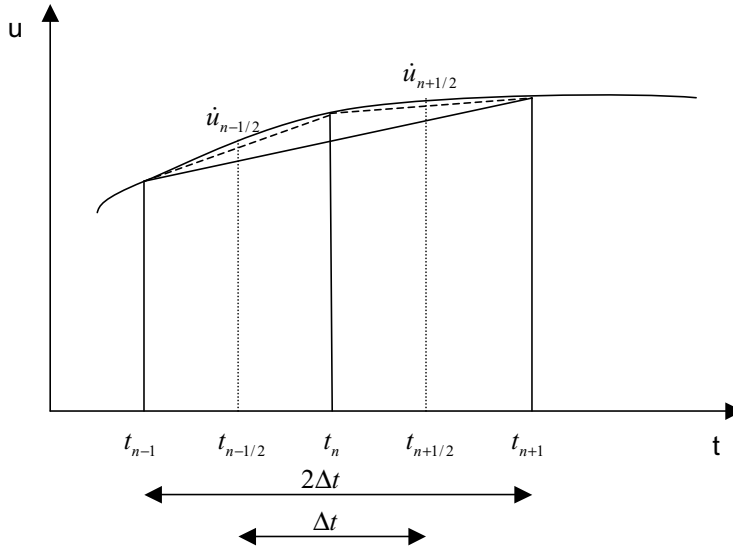


Figure 2.4: Central difference method (adopted from [3])

Now, at state n , both \dot{u}_n and \ddot{u}_n are functions of u_{n+1} . How this is applied when solving the equations of motions is also treated in Chapter 2.6.1.[5]

2.3 Shell elements

Shell elements can be regarded as plate bending elements combined with plane membrane elements. That is, a shell carries load both in the plane, membrane forces, and perpendicular to the surface. Shells can also have a curved surface, though, only flat linear elements are considered in this thesis. The definition of a thin shell is that its

thickness t is small compared to the overall dimensions. The thickness can be constant or vary within an element.

Consider the quadrilateral shell element in Figure 2.5a. The four corner nodes have 5 degrees of freedom each, 3 translations and 2 rotations.

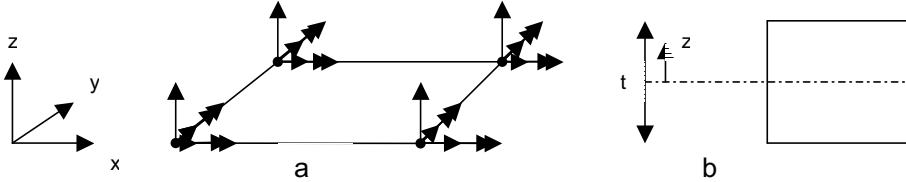


Figure 2.5: a) Quadrilateral shell element with d.o.f, b) Definition of midplane

The stresses in a shell generate membrane forces N , measured in force per unit length.

$$N_x = \int_{-t/2}^{t/2} \sigma_x dz; \quad N_y = \int_{-t/2}^{t/2} \sigma_y dz; \quad N_{xy} = \int_{-t/2}^{t/2} \sigma_{xy} dz \quad (2.28-2.30)$$

The stresses are calculated as a superposition of membrane and bending stresses. For a linear elastic thin shell the normal forces are independent of z and the bending stresses varies linearly with z .

$$\sigma_x = \frac{N_x}{t} + \frac{12M_x z}{t^3}; \quad \sigma_y = \frac{N_y}{t} + \frac{12M_y z}{t^3}; \quad \sigma_{xy} = \frac{N_{xy}}{t} + \frac{12M_{xy} z}{t^3}; \quad (2.30-2.32)$$

Stresses are evaluated at so called integration points within the element. An element needs 4 integration points to be stable, fully integrated. Elements with less integration points are called under-integrated. At every integration point a number of integration points through the thickness can be used to describe the stress variation. How under-integrated elements are treated is described in Chapter 2.6.2.[2]

2.4 Principle of virtual work

The energy principle is the base to the governing equations in the FE-method. A body is in static equilibrium when the internal energy is equal to the external according to the principle of virtual work:

$$\int_V \sigma_{ij} \delta \epsilon_{ij} dV = \int_V b_i \delta u_i dV + \int_S t_i \delta u_i dA \quad (2.33)$$

b_i is the body force, t_i is the surface force acting on the body and δu_i is a virtual displacement. This equation holds for large deformations as well if time history effects are considered. [8]

2.5 Adaptive method

With an adaptive solution one means that the FE-mesh is changing or refined continuously throughout the analysis. This change is due to, e.g. large deformation in certain areas where the initial mesh describes the geometry poorly. The aim with an adaptive method is to get the best accuracy at a minimum computational effort. When the optimal mesh changes during the analysis, as in non-linear analysis, the adaptive method gets even more beneficial. [7] Large deformation problems as metal forming are often analysed with an adaptive method.

To illustrate an adaptive process, consider the thin walled beam in Figure 2.6. In areas with large deformations the mesh needs to be refined to get improved accuracy. In other areas, where small or no displacements occur, the initial mesh describes the geometry well and therefore no refinement is necessary. [5]

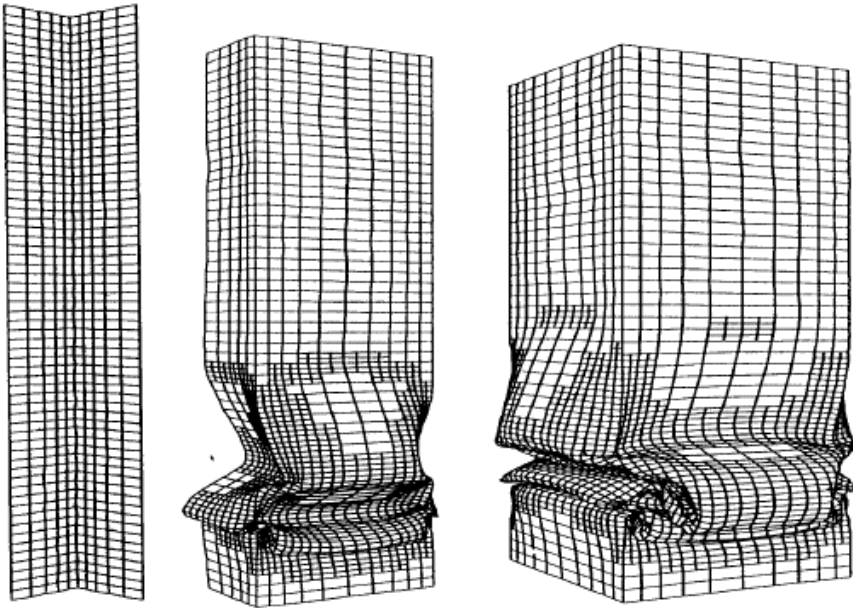


Figure 2.6: Thin cross section beam analysed with an h-adaptive method [5]

In Figure 2.6 the used h-adaptive method is based on a mesh refinement process. However there are other methods to increase the accuracy of a simulation. For example, the adaptive process can exist of increasing the polynomial order of the element

formulation. That is a linear element, for example, becomes a quadratic element after an adaptive refinement.

Generally, in an adaptive method the meshing procedure is based on error estimations. In the areas where the estimated error is too high, the FE-model is refined. In non-linear analysis the solution is obtained via load- or time steps. Therefore, error estimation has to be performed after each incremental step. Though, in practice, error estimation is performed at selected steps. The error estimation is based on the energy norm (difference between internal and external energy) within each element. Figure 2.7 shows an algorithmic scheme of a non-linear adaptive solution procedure. u , σ and ε are state variables such as displacement, stress and strain. i is the load step counter, k the iteration counter, m and n are mesh counters. After refinement the state variables must be mapped from the old FE-model to the new one. This is called rezoning. [7]

It should be mentioned that this is an example of a non-linear adaptive algorithm and not the algorithm used in LS-DYNA.

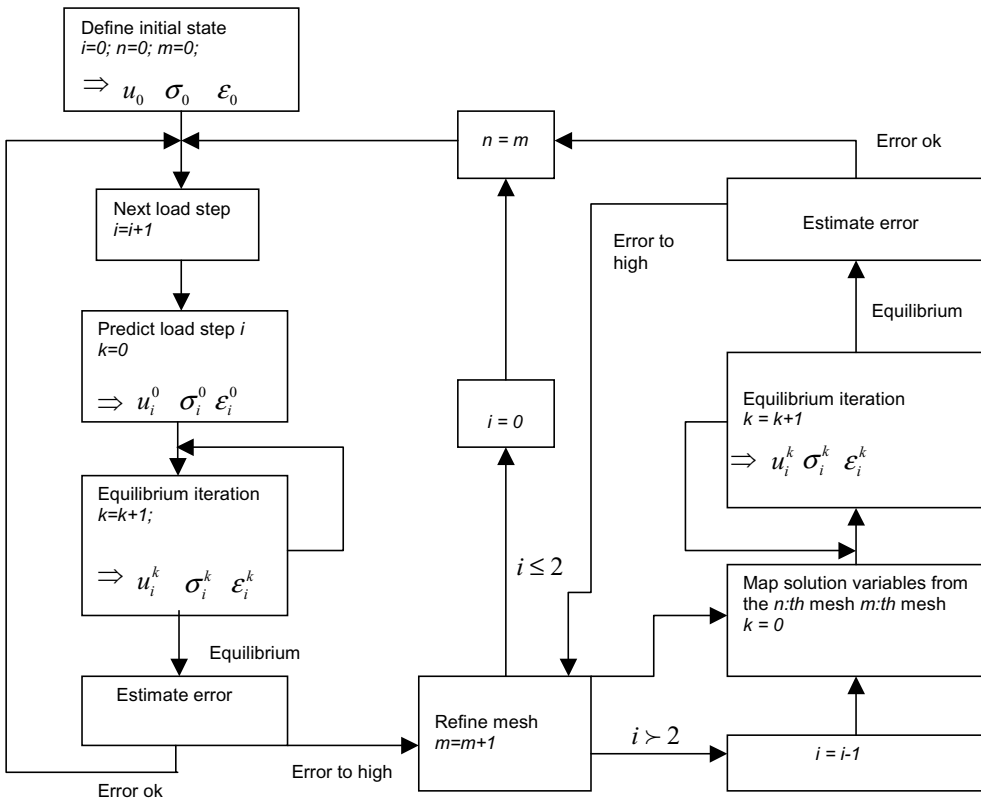


Figure 2.7: Algorithmic non-linear adaptive solution scheme (adopted from [7])

2.6 LS-DYNA

As mentioned in Chapter 2.1, LS-DYNA is an explicit FEM-program. It is appropriate to simulate fast dynamic problems, such as impact and shock problems. In this Chapter, the basics of the explicit time integration, program features and its properties are described.

2.6.1 Explicit time integration

As mentioned earlier LS-DYNA uses the central difference method to solve the equation of motion. The method has been described generally in Chapter 2.2. How DYNA handles the operations for an MDOF system is treated in this Chapter.

Earlier, the equation of motion has been formulated for an SDOF system. Now we want to formulate the relationships for an arbitrary number of DOF. In matrix form, the equation of motion appears as:

$$\mathbf{M}\ddot{\mathbf{u}} + \mathbf{C}\dot{\mathbf{u}} + \mathbf{f}^{\text{int}}(\mathbf{u}) = \mathbf{f}^{\text{ext}}(\mathbf{t}) \quad (2.34)$$

\mathbf{M} and \mathbf{C} have the dimensions $(dof \times dof)$, \mathbf{f} and \mathbf{u} have the dimensions $(dof \times 1)$. However, the formulation in LS-DYNA differs from the original equation. Because of the reduced integration that will be discussed in Chapter 2.6.2 an “hourglass” force is added. There might also be contact between different parts involved. Therefore a second force is added to the equation. How LS-DYNA handles these added forces numerically will not be treated in this thesis. For further reading, see [5] and [6]. Thus, the formulation in LS-DYNA appears as:

$$\mathbf{M}\ddot{\mathbf{u}} + \mathbf{C}\dot{\mathbf{u}} + \mathbf{f}^{\text{int}}(\mathbf{u}) = \mathbf{f}^{\text{ext}}(\mathbf{t}) + \mathbf{f}^{\text{hour}}(\mathbf{u}, \dot{\mathbf{u}}) + \mathbf{f}^{\text{cont}}(\mathbf{u}, \dot{\mathbf{u}}) \quad (2.35)$$

If we from now on disregard from “hourglass” and contact forces and return to the equation for an SDOF system, Equation 2.11. Inserting Equation 2.26 and 2.27 from the central difference method in Equation 2.11. The following expression appears:

$$\left(m + \frac{1}{2} 2\Delta t c \right) u_{n+1} = \left((\Delta t)^2 p_n - ((\Delta t)^2 k - 2m) u_n - \left(m - \frac{\Delta t}{2} c \right) u_{n-1} \right) \quad (2.36)$$

The only unknown is u_{n+1} , which is trivial to find by dividing the right side of Equation 2.36 with $\left(m + \frac{1}{2} 2\Delta t c \right)$. Now, consider this to be an MDOF system. Then, M is a matrix and therefore an inversion is necessary. In a system with a large number of DOFs this will be computationally expensive to do in every single time step. Therefore LS-DYNA uses a lumped mass matrix which has only non-zero values in the diagonal. Also the damping matrix is diagonal. The inversion of a diagonal matrix is trivial. A lumped mass matrix can be seen as every node obtaining a contribution which is proportional to the area of influence of the node as shown in Figure 2.8.

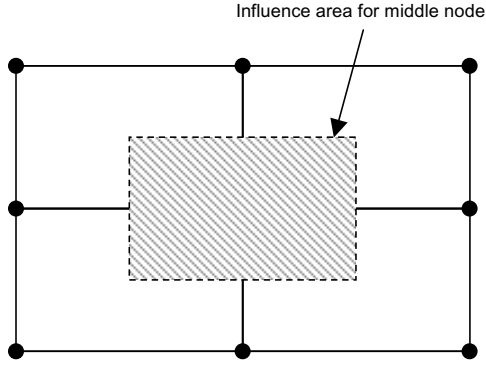


Figure 2.8: Influence area when calculating lumped masses

For the MDOF system the solution to u_{n+1} appears as:

$$\mathbf{u}_{n+1} = \left(\mathbf{M} + \frac{1}{2} 2\Delta t \mathbf{C} \right)^{-1} \left((\Delta t)^2 \mathbf{P}_n - ((\Delta t)^2 \mathbf{K} - 2\mathbf{M}) \mathbf{u}_n - \left(\mathbf{M} - \frac{\Delta t}{2} \mathbf{C} \right) \mathbf{u}_{n-1} \right) \quad (2.37)$$

The explicit time integration has many merits, it is memory efficient since no major matrix inverse operations need to be performed. It also makes it possible to describe a complex problem with a relative simple algorithm. However, it is as earlier described only conditionally stable which means that the time step may not exceed a critical value. This makes the explicit solver, as mentioned, appropriate for short time loading situations. If a slow process needs to be described, the computational effort will be too high. For example, the actual time to perform a metal forming may perhaps be 10 seconds but the simulations made in LS-DYNA are only performed during 50 ms. The critical time step, Δt_{cr} , depends on the size of the elements in the model. Small elements require a small time step to make the central difference method stable. [3] This critical time step is based on wave propagation. Basically it says that a wave can not pass an entire element in one time step. This leads to:

$$\Delta t_{cr} = \frac{L_{min}}{c} \quad (2.38)$$

Where L_{min} the shortest element side in the model and c is the so called wave propagation velocity, is calculated as:

$$c \approx \sqrt{\frac{E}{\rho}} \quad (2.39)$$

However, different methods can be used to increase the time step and also an implicit solver is included in LS-DYNA for slower processes. For further reading see [5]

2.6.2 Belytschko-Lin-Tsay shell

The most frequently used shell element is the so called *Belytschko-Lin-Tsay* element. It was first implemented in LS-DYNA as a computationally more efficient element than its precursor. It is considerably more efficient than the other types of shells and this advantage depends on several mathematical simplifications. However, because of these simplifications, it has some disadvantages. It loses stiffness considerably when it is warped and it is therefore not appropriate for analysing warped structures. Since only one integration point in the plane is used, zero energy modes may occur. The difference between an under integrated and a fully integrated element is shown in Figure 2.9a. Zero energy modes are also known as “hourglass” modes because of their shape. Two typical hourglass modes are shown in Figure 2.9b.

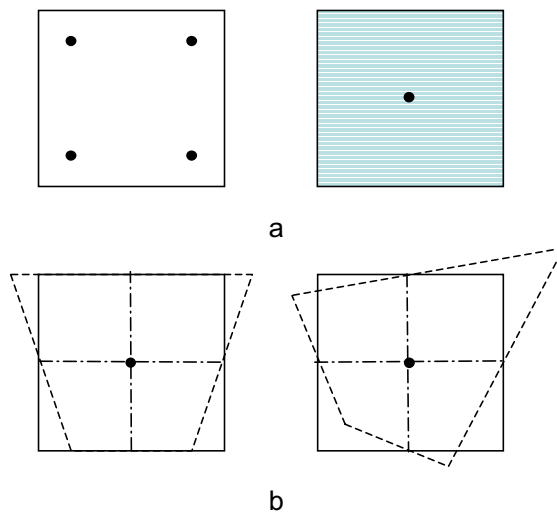


Figure 2.9: a) A fully integrated element to the left and a under integrated element to the right b) Two hourglass modes for the under integrated element

Since the strain is only evaluated in one point it is possible that no strains occur in that point. Therefore, the strain energy of the element is zero even though the element is considerably deformed. For a fully integrated element, the hourglass effect will not have an influence on the solution. As discussed earlier, an hourglass force is added to the equation of motion in LS-DYNA. The aim with this force is to control the formation of these modes. After the analysis, it is essential to control that the hourglass energy is small compared to the total energy. Otherwise, the solution will be inaccurate.

Displacements are only evaluated at the element nodes. The element is linear and therefore no bending deformation of the element is obtained within the element. An element formulation of higher degree would affect the critical time step considerably and is therefore rarely used in an explicit FEM-solver.[5] For further reading see [3] and [5].

2.6.3 Damping in LS-DYNA

LS-DYNA includes both Rayleigh and mass-proportional damping. For lower frequencies the mass-proportional damping is more efficient and therefore used. The damping is applied on the nodes of the deformable structure. The best damping is usually based on the critical damping of the lowest mode of interest. The damping affects both translations and rotations of the structure. The damping force is calculated as:

$$\mathbf{F}_{\text{damp}}^n = D_s \mathbf{M} \dot{\mathbf{u}} \quad (2.40)$$

Where D_s is a function of the lowest frequency of interest:

$$D_s = 2\omega_{\min} \quad (2.41)$$

With Equation 2.24 one can easily see that this refers to the critical damping for the lowest natural frequency. [5]

2.6.4 Contacts

The contact option in LS-DYNA treats interaction between different parts in a model. When different parts are interacting, forces appear in the contact interface. There are numbers of different contact options in LS-DYNA and the majority of them are based on the penalty method that will be treated later.

The contact used in this thesis is mainly a surface to surface contact, that is, one surface is impacting another surface. Node to surface and node to node contacts are other types of contact that work in a similar way. The surface to surface contact is computational more expensive than the other two but more stable and accurate when a coarse mesh is used. The contacts are usually defined by a master and a slave side. Generally the part with highest mesh density is used as a master side. Although, in the surface to surface contact the choice of master and slave side is arbitrary.

The penalty method consists of placing springs between all penetrating parts and the contact surface. How the penalty method works for a node to surface contact is illustrated in Figure 2.10

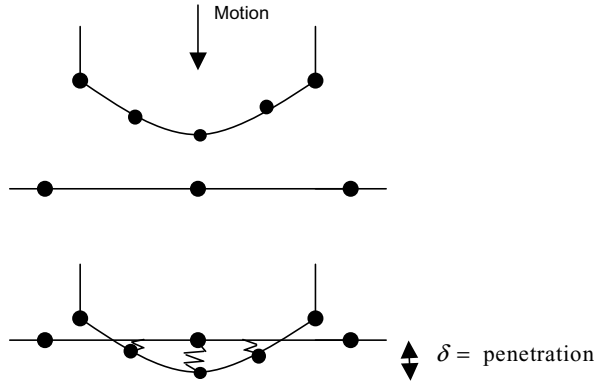


Figure 2.10: Penalty method (Adopted from [3])

The contact force is calculated as:

$$F = \delta k \tag{2.42}$$

Where k is the spring stiffness.

The surface to surface contact is treated symmetrically, that is, both master and slave nodes are checked against penetration. If the contact pressures become large, it is possible that unacceptable penetration occur. The method checks for initial penetration, that is, if a node already has penetrated a surface before the analysis starts. It is also possible to add friction and damping in the contact interface.[3]

2.6.5 Control volume

A way of controlling a simulation of an enclosed surface is to use a control volume. The enclosed surface can exist of shell or membrane elements and defines the control volume. By using the airbag card in LS-DYNA, the control volume can be exposed to a mass flow of a gas or liquid. That is, the structure is forced to expand as the enclosed volume is increased.

Consider for example a tube consisting of shell elements which defines the control volume and are exposed to a mass flow.

The enclosed mass in the volume can be calculated from:

$$M(t) = M(0) + \int_0^t \dot{M}_{in} dt - \int_0^t \dot{M}_{out} dt \tag{2.43}$$

\dot{M} denotes the mass flow per unit time, in and out of the enclosed volume respectively. The enclosed volume of the uncompressed liquid at a certain time can then be calculated as:

$$V_0(t) = \frac{M(t)}{\rho_0} \quad (2.44)$$

ρ_0 is the density of the uncompressed liquid. The volume of the fluid in the compressed state is calculated as:

$$V(t) = \frac{M(t)}{\rho} \quad (2.45)$$

The pressure generated by the mass flow and the current volume is calculated as:

$$P(t) = K(t) \ln \left(\frac{V_0(t)}{V(t)} \right) \quad (2.46)$$

Here, $K(t)$ is the bulk modulus. The pressure is uniformly applied on the surface within the control volume. [5]

In hydro-forming simulations, it is preferable to simulate the process with a control volume instead of using a linear pressure curve. The explanation to why this is preferable can be compared to a uniaxial tensile test. If the behaviour of the material is to be described in an appropriate manner, the test should be controlled by displacements and the force or stress be measured. Figure 2.11a illustrates a tube exposed to a mass flow which generates an internal pressure. The tube is surrounded by a rigid tool. The continuous line in Figure 2.11b illustrates the pressure generated by the mass flow as a function of the radius of the tube. That is the required pressure to form out the tube. The dashed line illustrates a linear pressure curve applied by the user.

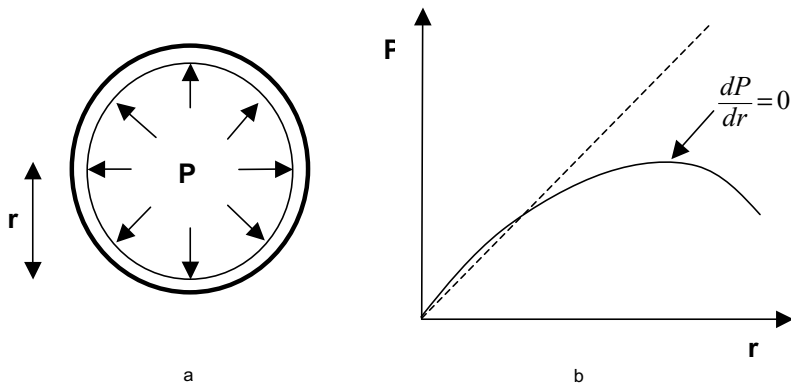


Figure 2.11: a) Tube exposed to a mass flow b) Obtained pressure by the flow and comparison to a linear pressure curve

A simulation with a control volume makes the process much smoother and no considerable dynamics effects are introduced. The simulation with a prescribed pressure makes the simulation unstable and dynamic effects are introduced. The critical state where $\frac{dP}{dr} = 0$ is not considered here.

2.6.6 H-adaptivity in LS-DYNA

As mentioned earlier there are different types of adaptive refinement processes. The major one used in LS-DYNA for shell elements is called h-adaptive. In this method the elements are subdivided into smaller elements whenever an indicator shows that a refinement of the mesh will provide improved accuracy of the solution. To decide the location of the areas needed to be refined, a *refinement indicator* is used. [5] Generally in adaptive methods, this indicator can be of several different types. Plastic strain rate, effective stress, change in thickness and relative change in angle between adjacent elements are examples of indicators. [7] The latter is shown in Figure 2.12.

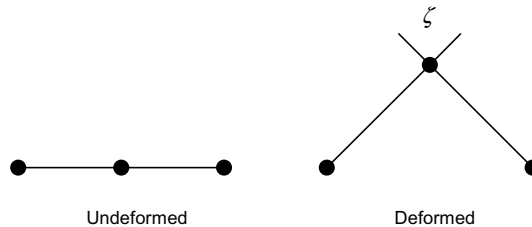


Figure 2.12: Change in angles as a refinement indicator (Adopted from [5])

The indicator used in LS-DYNA is based on change in angles for shell elements. The process when an element is divided into several smaller element is called *fission*. In h-adaptive methods the original element is divided into elements with sides $h/2$, where h is the characteristic size of the original element. In Figure 2.13, a quadrilateral is first divided into four quadrilaterals using the mid-points of the sides and the centre of the original element. The new elements can later be subdivided into smaller elements in several levels of adaptivity as shown.

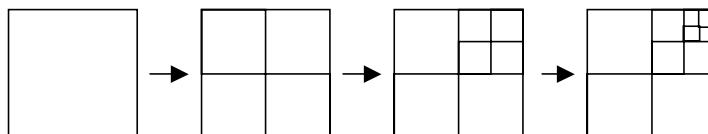


Figure 2.13: Fission of a quadrilateral element (Adopted from [5])

The adaptive process is automatic in LS-DYNA. The user sets the initial mesh, value of refinement indicator, update interval and maximum levels of adaptivity. The program subdivides those elements in which the refinement indicator has exceeded. This makes it possible to get an acceptable accuracy of a less computational resource than with a fix

mesh. Although, the process does not provide control of the error of the solution. The number of levels of adaptivity is though restricted by three rules:

1. The number of levels is restricted by the user. Normally, 3 to 4 levels.
2. In a mesh, the levels of adaptivity must be such that the levels of adaptivity in neighboring elements differ at most by one level.
3. The total number of elements in an analysis can be restricted by available memory.

Elements initially generated by the user are called parent elements. The new elements generated by the adaptive process are called *descendent elements* and the new nodes *descendent nodes*. The coordinates of the descendent nodes along the sides are generated by linear interpolation according to:

$$x_N = \frac{1}{2}(x_I + x_J) \quad (2.47)$$

Where x_N is the coordinate of the descendent node, x_I and x_J are the current node-coordinates along the side which the descendent node was generated.

The coordinate of the midpoint is generated in the same manner:

$$x_M = \frac{1}{4}(x_I + x_J + x_K + x_L) \quad (2.48)$$

Here, x_M is the descendent mid-point node and $x_{I,J,K,L}$ are the current nodes of the original element.

That is, the new node is placed in the plane that the parent element described and the bending deformation of the element is not considered.

Also velocities and angular velocities need to be described in the descendent nodes. Linear interpolation in the same manner as coordinates leads to:

$$v_N = \frac{1}{2}(v_I + v_J); \text{ Velocity of descendent node on the boundary.} \quad (2.49)$$

$$v_M = \frac{1}{4}(v_I + v_J + v_K + v_L); \text{ Velocity of descendent mid-point node.} \quad (2.50)$$

$$\omega_N = \frac{1}{2}(\omega_I + \omega_J); \text{ Angular velocity of descendent node on the boundary.} \quad (2.51)$$

$$\omega_M = \frac{1}{4}(\omega_I + \omega_J + \omega_K + \omega_L); \text{ Angular velocity of descendent mid-point node.} \quad (2.52)$$

The stresses and strains in the descendent elements are set equal to the state variables in the parent element at the corresponding through the thickness quadrature points.

Descendent nodes which are not corner nodes of an all attached element are treated as slave nodes and secondary conditions are applied to the present degrees of freedom.

When the new mesh is generated and the calculations can proceed the user has two alternatives;

1. Restart the calculations from actual state, one-pass adaptivity.
2. Back up to an earlier time state and repeat a part of the calculation with the new mesh, two-pass adaptivity.

The latter alternative is preferred for accuracy and stability reasons. The former is preferred for speed. The two alternatives are shown in Figure 2.14.

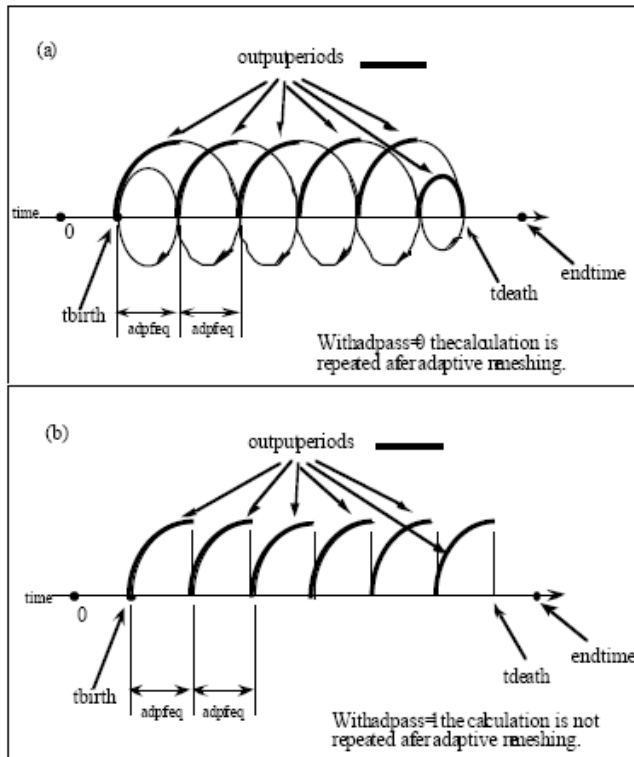


Figure 2.14: Alternatives after refinement of mesh a) Two-pass. b) One-pass [5]

Besides these two similar methods there is a third alternative adaptive method. It is called uniform adaptivity. This method refines the mesh at the initial state of the analysis. There is accordingly no indicator that needs to be exceeded. The number of elements will be increased but the method does not consider the geometrical aspects. [5]

3. Proposed method

In this chapter the methods and the procedure of the proposed h-adaptive method are described. Also the problems and properties for the present h-adaptive method are mentioned briefly.

3.1 Present adaptive method

As mentioned in the introduction, the problem with the present h-adaptive method is that the bending deformation of the element is not considered when the descendent nodes are generated. As described in Chapter 2.6.4, the descendent middle node is generated in the plane that the parent element described. This simplification of the geometry has proved to result in improper strains and strain distribution. This holds for all three types of adaptivity but it is most striking for the uniform and the one-pass adaptivity.

Later in this thesis two examples will be analysed with different adaptive methods. The described behaviour with the strain will then be presented more in detail.

3.2 About the proposed adaptive method

The fundamental basis of the new h-adaptive method is that the bending deformation of the shell element is to be considered when the mesh is refined. By this approach, the geometry of the structure is described in an improved manner. Consider the discrete element mesh of a curved surface in Figure 3.1a. With increasing nodal displacement, the mesh represents the true shape poorly. With the present adaptive method the descendent node is generated on the parent element. With the proposed method, this node is to be moved towards the true surface. Figure 3.1b illustrates the differences of the two methods.

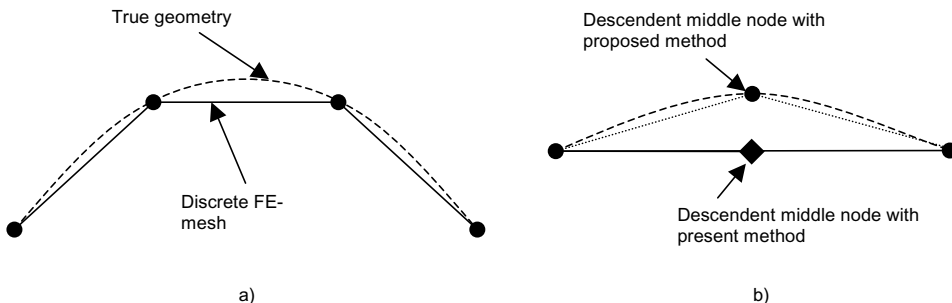


Figure 3.1: a) Discrete element mesh of a curved surface b) Difference between present and proposed location of descendent middle node

As mentioned in the introduction the proposed analysis method consists of several steps. Figure 3.1 illustrates the procedure during the analysis in LS-DYNA.

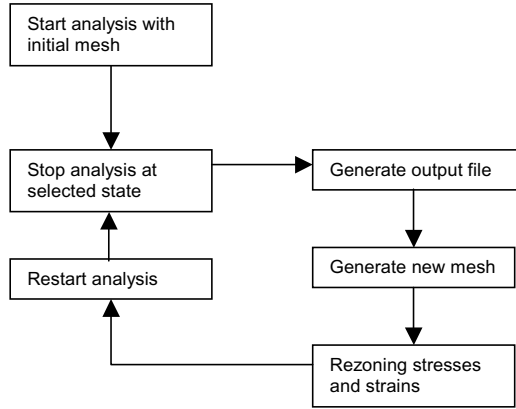


Figure 3.2: Analysis scheme in LS-DYNA for the proposed adaptive method

The initial mesh and the state when the analysis is stopped are defined by the user. With the command `*INTERFACE_SPRINGBACK_DYNA3D_THICKNESS`, LS-DYNA generates an output file containing nodal coordinates, stresses, strains and thickness of the elements. Next step in the procedure is to generate descendent nodes and create the new mesh. How the “true” shape is approximated is treated in the following chapter. When the new mesh is created all element history needs to be mapped from the parent to the descendent elements. The descendent elements are assigned the same state values as the corresponding parent element, as in the present method. The analysis can now be restarted and the adaptive procedure can be repeated any desired number of times. This new method will only be evaluated as a one-pass method. However, it is possible to make the new method work as the present two-pass method.

There is a drawback though to the proposed procedure. Since the method performs a virtual displacement of the generated descendent node that is not a result of an external force, one automatically has added energy to the system. This energy is however not taken into consideration in the principle of virtual work. This may lead to a loss of total energy of the system in the end. If the conservation of energy between the parent and the descendent elements should hold, one has to adjust the stresses. Consider the principle of virtual work, Equation 2.33, with the modification that one neglects the body forces.

$$\int_V \sigma_{ij} \delta \epsilon_{ij} dV = \int_S t_i \delta u_i dA \quad (3.1)$$

At a certain state, this equilibrium is fulfilled. When introducing the descendent node as in the present method the equilibrium holds. Consider now that the middle node is moved to the approximated surface. One has introduced a virtual displacement Δu_i of certain nodes which should lead to an incremental change in external work, right side of Equation 3.1. t_i , σ and ϵ are constant at this state and it should lead to that the equation of equilibrium is not fulfilled.

$$\int_V \sigma_{ij} \delta \epsilon_{ij} dV \neq \int_S t_i \delta u_i dA \quad (3.2)$$

Unless, there is an adjustment to σ_{ij} , the energy between the parent and the descendent elements will not be conserved.

However, the method described in this thesis is not based on conservation of energy and a loss of energy in the simulation will not be adjusted in any way. This may lead to inaccurate results with respect to stresses. This effect will be discussed later in Chapter 5 and 6.

3.3 Approximating shape in 2 dimensions

The base in the new method is to describe the “true” shape of a deformed structure by the nodal displacement. At a certain step in the analysis the mesh needs to be refined. Now, the approximated shape has to be described. The new geometry is expressed by each element in a local coordinate system, $(\bar{x}, \bar{\delta})$, shown in Figure 3.3

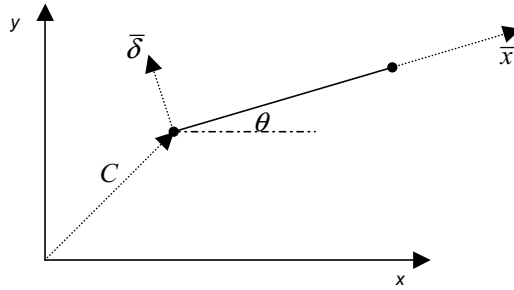


Figure 3.3: Definition of local coordinate system for an element

The relation between the local $(\bar{x}, \bar{\delta})$ and the global (x,y) coordinate system for a coordinate P , can be expressed as:

$$\begin{bmatrix} \bar{x} \\ \bar{\delta} \end{bmatrix} = \begin{bmatrix} \cos(\theta) & \sin(\theta) \\ -\sin(\theta) & \cos(\theta) \end{bmatrix} (P - C) \quad (3.3)$$

The approximating function which describes the shape is of the third degree in the 2-dimensional case. That is:

$$\bar{\delta}(\bar{x}) = \alpha_1 + \alpha_2 \bar{x} + \alpha_3 \bar{x}^2 + \alpha_4 \bar{x}^3 \quad (3.4)$$

To be able to determine the constants α one needs four boundary conditions, the nodal normal and the nodal values. This normal is calculated as an average of two neighbouring elements normal. Figure 3.4 illustrates the definitions.

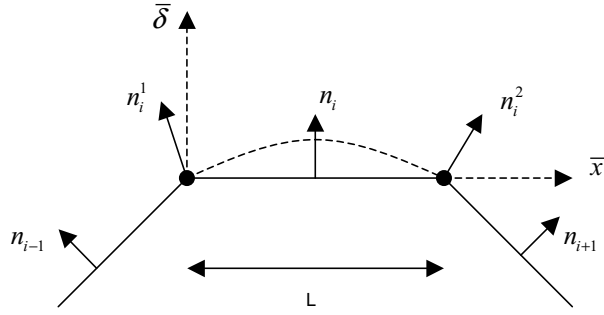


Figure 3.4: Element normal and calculated nodal normal

The nodal normal can now be calculated as:

$$n_i^1 = \frac{1}{2}(n_{i-1} + n_i), \quad n_i^2 = \frac{1}{2}(n_{i+1} + n_i) \quad (3.5)$$

With the nodal values and the normals one can now find the constants in Equation 3.4. The slope in the nodes is orthogonal to the normal. In matrix form, Equation 3.4, leads to:

$$\mathbf{A}\mathbf{a} = \mathbf{b} \rightarrow \begin{bmatrix} 1 & \bar{x}_1 & \bar{x}_1^2 & \bar{x}_1^3 \\ 0 & 1 & 2\bar{x}_1 & 3\bar{x}_1^2 \\ 1 & \bar{x}_2 & \bar{x}_2^2 & \bar{x}_2^3 \\ 0 & 1 & 2\bar{x}_2 & 3\bar{x}_2^2 \end{bmatrix} \begin{bmatrix} \alpha_1 \\ \alpha_2 \\ \alpha_3 \\ \alpha_4 \end{bmatrix} = \begin{bmatrix} \bar{\delta}(\bar{x}=0) \\ \left. \frac{d\bar{\delta}}{d\bar{x}} \right|_{\bar{x}=0} \\ \bar{\delta}(\bar{x}=L) \\ \left. \frac{d\bar{\delta}}{d\bar{x}} \right|_{\bar{x}=L} \end{bmatrix} \quad (3.6)$$

The vector \mathbf{a} is calculated as:

$$\mathbf{a} = \mathbf{A}^{-1}\mathbf{b} \quad (3.7)$$

Now, the shape is determined and the location of the descendent node can easily be determined in the local coordinate system and also transformed to the global system. The descendent node is always generated in the centre of the original element, that is, at $\bar{x} = L/2$.

The new geometry is generated by a function written in MATLAB, see Appendix A.

4. Introductory examples

In this chapter, two minor examples are given to see how variables can be transferred from one FE-model to another and if the new method appears to work in a satisfying way.

4.1 Linear elastic beam

The aim with considering a linear elastic simple beam model is to see how the nodal displacements change with an increasing number of elements. Also, one can study how a set of displacements can be transferred from a model with few elements to a new model with more elements. Consider the beam with a distributed load in Figure 4.1. If one considers only nodal displacement and no bending of the element segments, one obtains the displacement as shown below.

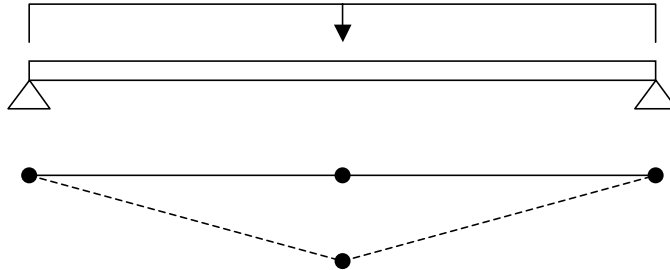


Figure 4.1: 2-element beam with distributed load and the corresponding nodal displacement

With only two elements we get the displacement at the mid-node as shown in Figure 4.1. By refinement a new node is inserted in the centre of the origin element. By symmetry reasons one can study the geometry shown in Figure 4.2.

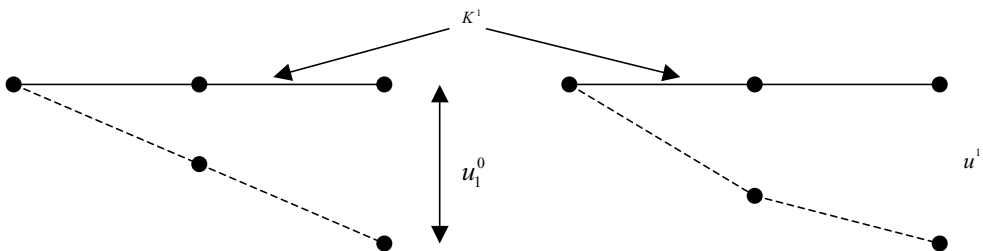


Figure 4.2: New middle node is introduced and the new nodal displacements \mathbf{u}^1

With the displacement inserted from the old model, the new nodal loads and the stiffness calculated from the initial state (horizontal) one obtains the following relationship:

$$\mathbf{K}^1 \mathbf{u}^0 - \mathbf{f}^1 = \mathbf{r} \quad (4.1)$$

Here, \mathbf{K}^1 is the new stiffness and \mathbf{r} is the error. To get the new displacements, \mathbf{u}^1 , one needs to add $\Delta \mathbf{u}$, which is calculated as:

$$\Delta \mathbf{u} = \mathbf{K}^{-1(0)} \mathbf{r} \quad (4.2)$$

Since, it is not possible to invert \mathbf{K} one needs the boundary conditions and thereafter invert the reduced \mathbf{K} . The total displacement for the new model is:

$$\mathbf{u}^1 = \mathbf{u}^0 + \Delta \mathbf{u} \quad (4.3)$$

These studies are made to understand how variables can be mapped from one FE-model to another. In the following examples stresses and strains will be mapped from one model to another.

4.2 Shell strip

In this chapter a thin shell strip is considered in LS-DYNA. The aim with this example is to see how the energy differs for different types of approaches and verify that the proposed method is accurate enough. The strip is supported at its both ends and it is exposed to a uniform pressure which during the analysis operates perpendicular to the shell. The models below have been analysed.

1. An initial fine mesh consisting of 8 elements.
2. An initial mesh of 2 elements is used with the present two-pass adaptive method to refine the mesh 2 levels up to 8 elements.
3. An initial mesh of 2 elements is used with the present one-pass adaptive method to refine the mesh 2 levels up to 8 elements.
4. An initial mesh of 2 elements is used with the new adaptive method to refine the mesh up to 8 elements.

The strip was loaded such that plastic strain was initialized. The material properties for the steel used are shown in Appendix B.

In these analyses, the damping described in Chapter 2.6.3 is applied. The lowest angular frequency is calculated according to beam theory.

$$\omega_n = (\pi L)^2 \sqrt{\frac{EI}{mL^4}} \quad (4.4)$$

The first analysis with 8 elements is used as a reference when comparing the other methods. In analysis with the present h-adaptive method, a relative change in angles of 3 degrees is used as a refinement indicator.

For the new adaptive method, the two refinements have been made continuously over the load curve. The refinement procedure follows the described process in Chapter 3.2. The results for the three different analyses are shown in Table 4.1.

Table 4.1: Results for the four different analyses

Variables	Initial 8 elements	Present two-pass adaptive	Present one-pass adaptive	New adaptive
Deflection of middle node (mm)	-304	-304	-342	-308
Deflection at $x=L/4$ (mm)	-227	-	-	-230
Total energy (MNm)	28,3	28,7	37,3	26,2
Internal Energy (MNm)	28	28,15	36,2	26
Max. eff. stress in middle section (MPa)	253,3	253	253	250,8
Max. eff. strain in middle section	-	-	-	-
Upper surface	0,0573	0,0588	0,062	0,0582
Mid surface	0,0585	0,05885	0,074	0,0593
Lower surface	0,0599	0,0594	0,085	0,0606

From Table 4.1 one can distinguish that the present one-pass method separates from the other three analyses. The new method on the other hand, shows decent accuracy compared to the reference and the present two-pass method. However, there is a certain loss in internal energy for the new adaptive method, even if it is only about 7%.

It should be mentioned that it is the most interesting case to compare the present one-pass method and the new method, since it is also a kind of one-pass method. It is not possible to compare the total CPU-time for these two analyses since the new method is performed by hand but it can be interesting to compare the time for the two present methods to get an understanding how much more effort the two-pass method claims. The total CPU-time for the two adaptive simulations is as follows:

- one-pass: 39 s
- two-pass: 100 s

It is not straightforward to claim that the new one-pass method will have the same low computational cost as the present one-pass method but it is most likely that the new method will be more efficient than the present two-pass method. After all, it shows comparable accuracy to the two-pass method.

5. Hydro-forming analyses

In this chapter two examples are analysed to distinguish the differences between a reference solution, a solution with the present adaptive method and one with the new adaptive method. The analyses are similar to each other. Both are simulations of a hydro-forming process of a tube and the main theme is that the tube is somehow formed into a radius. The first example may not have a great practical use but it is uncomplicated to analyse and to compare the results. In the second example, the adaptive method is used in a more relevant problem that is likely to occur in the metal-forming industry. Also some other problems that occurred with the present adaptive method will be discussed. As mentioned earlier the focus is to distinguish differences in plastic strain and its distribution. As mentioned in Chapter 3.2, changes in total energy lead to incorrect stresses. Therefore, the internal energies will be compared and how this affects the stresses.

Both analyses are modelled with a surrounding rigid tool. Because of stability reasons, the analysis is made by using the earlier mentioned mass flow instead of an internal pressure. As described in Chapter 2.6.5 this makes the deformation progress much smoother. In the two examples the default Belytschko-Lin-Tsay shell element is used. The material properties for the aluminium are shown in Appendix B.

5.1 Expanding tube

In this first example the tube is surrounded by a rigid cylinder, a tool, of greater radius than the tube. With a constant mass flow into the volume, the cylinder expands symmetrically and forms out to the rigid form. The dimensions of the model are shown in Figure 5.1. With this specific geometry some problems occur with the earlier described surface to surface contact. Then the tube has initiated contact with the tool it starts to rotate in the cylinder due to its faceted FE-surface. This behaviour affects the results and makes them unreliable and the analysis loses its purpose. Therefore another type of contact is applied to the problem, called contact entity. How this contact works will not be treated in this thesis. For further reading see [5]. However, this specific contact showed to perform poorly with the present adaptive method. This will be explained later. To avoid the unwanted rotation of the tube friction was applied in the contact surface to surface interface. However this also resulted in improper strains.

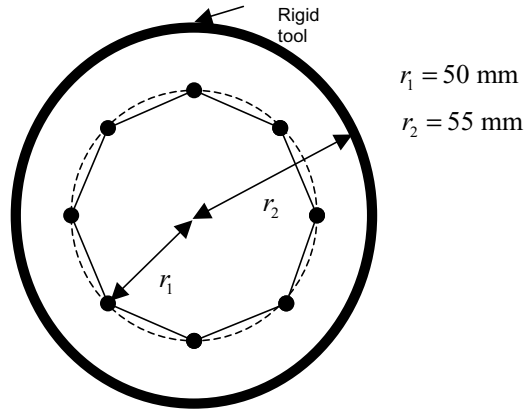


Figure 5.1: Analysed cylinder

The length of the tube is 180 mm and the initial thickness of the shells is 2 mm. The process is simulated during 10 ms. For the adaptive analysis, the initial mesh consisted of only 8 elements and 2 levels of adaptivity were applied, see Figure 5.1.

The following different analyses are to be compared.

- A reference analysis with an initial fine mesh, i.e. 32 elements
- The present one-pass adaptive method
- Uniform adaptivity
- The new adaptive method

5.1.1 Analyses

The first analysis is made with an initial fine mesh and no adaptivity is applied. This analysis is made as a reference. Since the tube expands symmetrically a uniform strain distribution is expected. This is why the current example is appropriate for distinguishing differences in the analyses.

As mentioned earlier some problems occurred when combining the present adaptive method with the current contact. The descendent nodes started to penetrate the rigid form considerably and this led to inaccurate results. To avoid this, the simulation had to be stopped after each mesh refinement. A complete result file was written and then the simulation was restarted with the result file included. Therefore, only the present one-pass adaptive method is analysed since it would be demanding to back up to an earlier state and restart the analysis like in the two-pass method. It is the author's opinion that this penetration depended on some problems with the updating of the descendent nodes.

Since the adaptive refinement is based on a change in angles between neighbouring elements the model has to be triggered to perform a mesh refinement. Consider the FE-mesh in Figure 5.1. If this model starts to expand symmetrically, no change in angles will occur during the whole analysis. The cylindrical geometry will be intact, only the

enclosing volume will increase. Therefore, the first mesh refinement is performed initially, see Figure 5.2. That is, the initial model actually consists of 16 elements. Now, the nodal displacements will lead to change in angles and another mesh refinement will be performed when the change in angle is 2 degrees. The first refinement can be compared to the uniform adaptivity that also will be analysed.

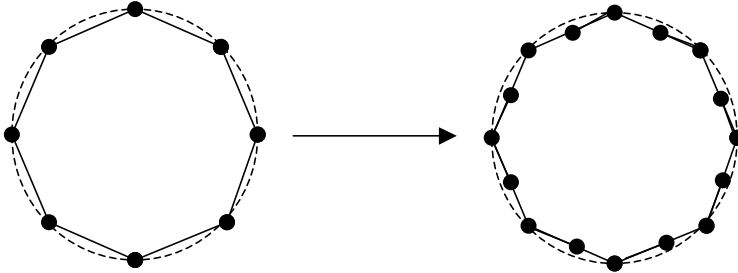


Figure 5.2: First mesh refinement at initial state to trigger of the adaptive procedure

One analysis is made with the present uniform adaptive method. In the first two steps the mesh is refined first to 16 elements and then to 32 elements. Also in this analysis, the simulation was stopped after the second refinement and thereafter restarted with an included result file.

With the new method, the mesh initially consisted of 8 elements. The mesh refinement was made by hand after the simulation was had terminated. The procedure for the analysis follows the scheme in Figure 3.2. The refinements have been made at two arbitrary points in time.

5.1.2 Results

As expected the reference analysis proved a homogenous strain distribution in the whole model. The initial mesh was therefore fine enough to achieve a representative result. The results are shown in Table 5.1.

Table 5.1: Effective plastic strain values for the different analyses

Variables	Reference analysis	New adaptive method	Present one-pass	Present uniform
Max. effective plastic strain in the model (%)	11,1	12,8	21,5	21,3
Min. effective plastic strain in the model (%)	11,1	12,2	21,1	20,4

The noticeable with this simulation is that the present adaptive method totally failed. The strain distribution is rather homogenous but, the absolute maximum value is almost twice the value calculated with the reference model. This holds both for the one-pass as well as the uniform method. The new adaptive method performed considerably much better than the present. The strain distribution is not completely homogenous but the strain absolute maximum value differs only by 1.7%.

Regarding the internal energies it is not possible to evaluate the present one-pass method since it was performed in several steps, but for the other analyses the following results were obtained:

- Reference analysis: 1.19 MNm
- Uniform adaptive analysis: 1.83 MNm
- New adaptive method: 1.13 MNm

The uniform adaptive method showed high internal energy compared to the reference model. For the new method, the energy is close to the reference model. However, since the strains were slightly too high this leads to low stresses according to the principle of virtual work.

5.2 Hydro-forming of a tube

This example is much similar to the first one, but now the tube is expanding and formed into a square-shaped tool with curved corners. In the first example, the present adaptive method showed inaccurate strains but the distribution was uniform through the model. The new method will now be compared to a reference model and to the present adaptive method for a more complex geometry. The model and its dimensions are shown in Figure 5.3.

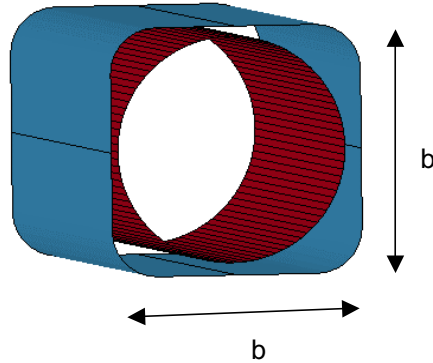


Figure 5.3: Geometry and dimensions of the tube and the rigid form

The sides of the square, b , are 55 mm. The initial radius of the tube is 50 mm. This simulation has been made with different values on the radius of the corners. The results are presented for a simulation with radius of 20 mm. Also radiuses of 10 mm and 30 mm have been analysed. The differences for these analyses will be mentioned later. Also this simulation is performed during 10 ms and 2 degrees are used as a refinement indicator.

A control volume is used also in this simulation. Since the tube is incapable to rotate inside of the tube in this case the surface to surface contact can be used. To really make the tube stick, a coefficient of friction of 0.1 is applied on the contact interface. With this contact, the present adaptive method functions well and no restarts are necessary. In this simulation a higher mesh density of the model is necessary to obtain an accurate result. Therefore an initial finer mesh than in the previous simulation is used. The following models have been analysed:

- A reference analysis with 96 elements.
- The present two-pass adaptive method. Starting with 24 elements and applying two levels of adaptivity.
- The present one-pass adaptive method with the same properties as the former.
- The present uniform adaptive method with the same properties as the former.
- The new adaptive method. Starting with 24 elements and refined twice at the same state as the two-pass method.

Besides comparing absolute strain and its distribution, the internal energy is to be compared.

5.2.1 Analyses

For the reference analysis the expected result is not that easy to predict as in the previous analysis. One can expect high and homogenous strains through out the whole radius. In the other areas, one can not predict the results except a symmetric strain distribution in the tube.

As described earlier for the two-pass method, the initial mesh consisted of 24 elements and the model is refined twice to a final state consisting of 96 elements around the tube.

The adaptive refinement indicator control is performed every 1 ms, that is ten times during the simulation. For stability reasons, the time step is scaled with a factor 0.4.

The one-pass simulation is the most interesting one to compare with the new adaptive method since the new one, as used here, also is a one-pass adaptive method. The same properties hold for this simulation as for the two-pass analysis. However, this method showed some instability problems in spite of the fact that the time step was scaled. This will be discussed later.

The uniform analysis is not of major interest to compare with the new method since it is a completely different type of method. It is still relevant to see how this method differs from the two-pass method and distinguish a certain behaviour. The time step was scaled with a factor 0.7 to avoid contact instability.

The simulation with the new adaptive method is performed in the same manner as in the previous example, but the model is refined at the same time states as for the two-pass adaptive method.

5.2.2 Results

The reference solution showed a homogenous strain distribution through the radius and a symmetric strain distribution in other parts of the model. A final model of 96 elements should therefore be fine enough to show accurate results. The maximum strain in the radius is 40.6% and the minimum strain in other parts of the model is 20.9%. The maximum and minimum strain values for the different analyses are presented in Table 5.2.

It should be mentioned that the present one-pass adaptive method showed contact instability even though the time step was scaled with a factor 0.05. Therefore, no results will be presented for the one-pass analysis.

Table 5.2: Absolute strain values for the different analyses

Variables	Reference analyse	New adaptive method	Present two-pass	Present uniform
Max. plastic strain in the model (radius) (%)	40,6	38,1	43,3	43,5
Min. plastic strain in the model (%)	20,9	23,1	21,1	22,7
Internal energy (MNm)	3,95	3,25	3,98	3,98
1:st principal stress (MPa)	210	154	217	218

The adaptive analyses showed comparable accuracy with respect to maximum strain in the radius. However, the new adaptive method showed lower maximum strain in the radius and higher minimum strain in other parts of the model. The present adaptive method showed both higher maximum and minimum strain. The absolute strain value is not of greatest interest when comparing the two methods but it is of importance that the simulation shows acceptable accuracy.

When it comes to the strain distribution in the radius the different analyses differs. The two-pass and the uniform method show an inhomogeneous strain distribution in the radius. For the uniform method, the behaviour is the most striking. The new method, on the other hand, showed a completely homogenous strain distribution. This holds for the analyses with 10 and 30 mm radius as well. Figure 5.4 illustrates the inhomogeneous distribution for the present two-pass adaptive method to the left and the new adaptive method to the right.

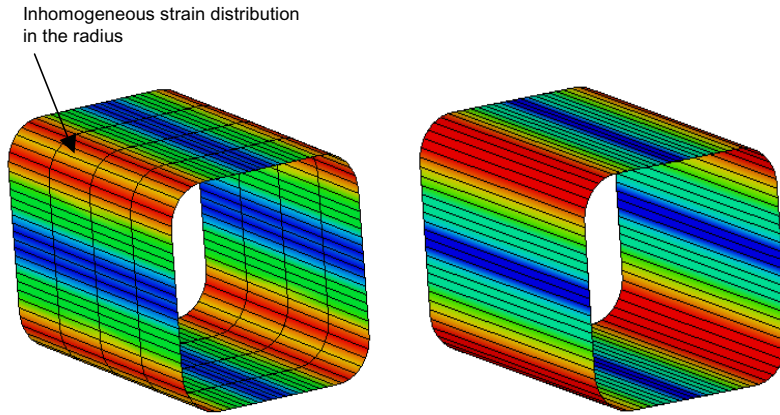


Figure 5.4: Strain distribution for the present two-pass adaptive method to the left and the new adaptive method to the right

In Figure 5.5, the strain along the middle section is plotted for the four compared analyses. The starting point is in the centre of the radius.

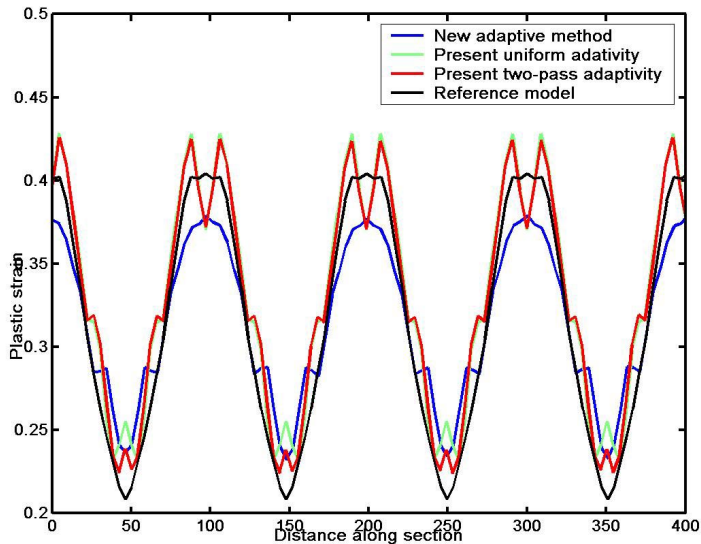


Figure 5.5: Strains along the section for the different analyses

From Figure 5.5 one can easily observe the inhomogeneous strain behaviour of the present adaptive method. The peaks illustrate the strain in the radius and there is a clearly visible V-shaped peak for the two analyses with the present adaptive method (red and green curve). For the new adaptive method no such behaviour is visible. As mentioned earlier, it is the absolute strain values that differ from each other. In Figure 5.6, only the new method is compared to the reference model.

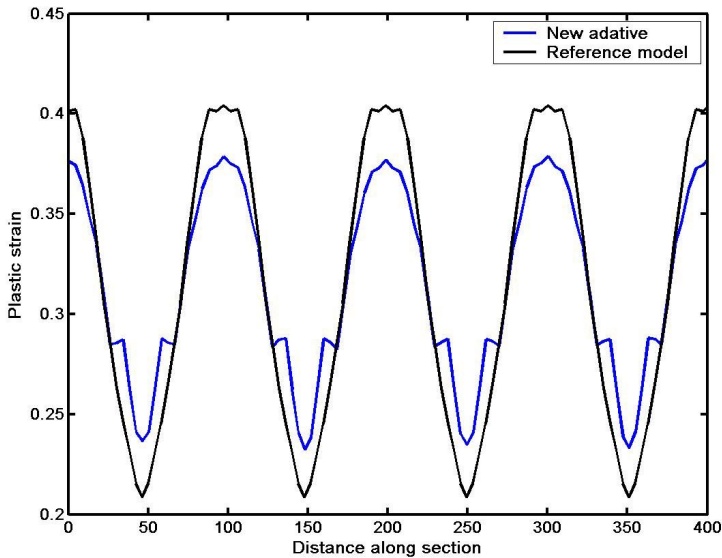


Figure 5.6: The reference analysis compared to the new method.

Even if the plotted curves in Figure 5.6 are not completely correlated the new method proves a more accurate behaviour than the present adaptive method.

When it comes to the internal energy for the analyses it is clearly visible that there is a loss in internal energy for the new method. The calculated stresses are, due to the energy losses, too low compared to the reference model.

All the adaptive analyses have common strain behaviour with the sharp notch, only at different positions. Why the adaptive analyses prove this behaviour is hard to explain.

6. Discussion of results

This chapter will discuss the results and experience from the different examples. The conclusions are based on the two examples that have been presented in the thesis. Other opinions are based on the author's experience of the analysed examples and own assumptions.

6.1 Discussion of the hydro-forming examples

For a start, it should be mentioned that the results of the examples performed in this thesis can not in any way represent a general behaviour of the new method. However, these examples demonstrates how well the new method performs in these particular cases and one can make own assumptions on the behaviour of an arbitrary structure and some general conclusions can be drawn, though. This will be discussed later.

In the first hydro-forming simulation with the expanding tube the new method proved to perform considerably much better than the present. Exactly why the present adaptive method generates these inaccurate results is hard to tell but it is the author's opinion that it depends on the poorly described geometry. As described in Chapter 2.6.6 the descendent node is generated on the same plane as the parent nodes and the bending of the element is not considered. Consequently, after each mesh refinement the simulation is restarted with the wrong geometry. In the uniform case it is particularly easy to see the incorrect description of the geometry. If Figure 5.2 is considered, one can see that the refinement describes the tube as poor as the initial mesh did, only the number of elements has been increased. Though, in practice, it is the same case with the one-pass method. It is possible that the two-pass method would perform better but it is most likely that even that method would fail. In particular, these inaccurate results may be noticeable when the initial mesh is as coarse as it was in these simulations and the structure is strongly curved. However, both the present and the new adaptive method showed a homogeneous strain distribution.

The uniform adaptive method showed higher internal energy than the new adaptive method as well as the reference model. This is also due to the geometrical simplification with the present method and the fact that the initial mesh was rather coarse. The new method on the other hand showed a comparable internal energy with the reference analysis despite the coarse mesh. That the difference in energy was insignificant for this case may depend on the states where the model was refined.

For the second hydro-forming analysis the differences of the simulations are of another kind. The absolute strain values are comparable with the reference simulation both for the present and for the new adaptive method. However, the new adaptive method eliminated the unwanted behaviour with inhomogeneous strains in the radius, which was one of the primary aims with the method.

The drawback with the new method is obviously the losses of internal energies. The losses depend, as described in Chapter 3.2, on the virtual displacement of the descendent node which is not included in the principle of virtual work. This leads to a loss of external work and accordingly to a loss of internal energy. These losses lead to inaccurate stresses.

In this example the present adaptive method proved comparable internal energy with the reference model. This may be due to the relatively fine initial mesh. However, the author expected that the uniform adaptive method would lead to high internal energy also in this case.

6.2 Future development of the method

As mentioned earlier the new method improves the solution accuracy in terms of strain and its strain distribution. To really investigate how the new method performs in a larger scale, it has to be implemented in LS-DYNA. However, the problems with the internal energies have to be solved. That is the virtual displacement of the descendent node has to be included in the principle of virtual work. How the computational effort would differ from the present one-pass method is difficult to predict but it is the author's opinion that it would not be striking since the element normal is calculated at every state in the analysis.

It could be an interesting task to investigate how a similar two-pass method would perform compared to the new one-pass method.

The next natural step would also be to implement the method for three dimensional cases. This will of course take more efforts but is necessary for the practical use of the proposed method.

Outside the range of this thesis it would also be of an interest to investigate why different types of adaptivity failed with a specific contact. Also, a closer investigation on how hydro-forming simulations can be modelled in a better manner and which contacts that are most appropriate to use.

7. Conclusions

The drawback with the present method is that the refined geometry is poorly. Consequently, after each refinement the analysis restarts with an incorrect geometry. This is in particular noticeable for the one-pass and the uniform adaptive methods. Inaccurate strains and corresponding strain distribution are results of this geometrical simplification. This will in some cases also lead to higher external energies than expected and therefore inaccurate stresses.

The final conclusions of the new method for the analysed examples are:

- Improved accuracy in terms of strains compared to the present uniform, one-pass as well as the two-pass method.
- Improved strain distribution compared to the other present adaptive methods.
- Probably more effective than the present two-pass method. That is, improved accuracy in terms of strains of a lower computational effort.
- Loss of internal energy, which leads to inaccurate stresses.

The third conclusion is based on the results for the new method combined with the difference in total CPU-time for the present one-pass and two-pass method. This statement depends on how effective the new mesh generator is implemented.

Further, how accurate the internal energies are, and hence the stresses, appears to depend on:

- Element density of the initial mesh.
- The degree of curvature of the structure.
- At which state the mesh refinement is performed.

A combination of a rough mesh and a strongly curved surface generates a large virtual displacement and therefore a large loss of internal energy is expected. A mesh refinement early in the analysis, when the displacements are minor, should lead to smaller losses in energy. However, for the last case the adaptive method has lost its purpose.

References

- [1]. Chopra, Anil K., *Dynamics of structure*, 2nd ed., Prentice Hall, New Jersey, 2001
- [2]. Cook, Robert D. et al., *Concepts and applications of finite element analysis*, 4th ed, Wiley, 2002
- [3]. Engineering Research AB, *LS-DYNA introductory course*, 2005
- [4]. Heath, Michael T., *Scientific computing. An introductory survey*, 2nd ed., McGraw Hill, 2002
- [5]. Hallquist, John O., *LS-DYNA 970 theoretical manual*, Livermore Software Technology Corporation, Livermore, 2003
- [6]. Hallquist, John O., *LS-DYNA 970 keyword user's manual*, Livermore Software Technology Corporation, Livermore, 2003
- [7]. Okstad, K.M. and Mathisen, K.M., *Towards automatic adaptive geometrically non-linear shell analysis, Part 1: Implementation of an h-adaptive mesh refinement procedure*, International Journal For Numerical Methods In Engineering, vol 37, 1994, pp. 2657-2678
- [8]. Sundström, Bengt et al., *Handbok och formelsamling i hållfasthetslära*, Institutionen för hållfasthetslära KTH, Fingraf AB, 1999

Appendix A

Function for generate descendent node-coordinates

```
function GlobalCoord=shapefunc(X,Y);

%-----
% PURPOSE
% Approximates a function of degree 3 that intersects all
% nodes specified in X & Y. Generates new nodes on the curve in the
% middle of the two original nodes to create a refined mesh. The input has
% to be continuously and the structure non-enclosed.
%
% INPUT: X = [x1 x2 x3...xn]' node coordinates (continuously)
%         Y = [y1 y2 y3...yn]' node coordinates (continuously)
%
% OUTPUT: GlobalCoord = Generated node coordinates in order.
%         [x1_new y1_new
%          x2_new y2_new
%          .....]
%-----

nnd=length(X);
nel=nnd-1;
GlobalCoord=[];

for i=1:nel

    Li=sqrt((X(i)-X(i+1))^2+(Y(i)-Y(i+1))^2);
    C_0=[X(i);Y(i)];

    A=[1 0 0 0
        0 1 0 0
        1 Li Li^2 Li^3
        0 1 2*Li 3*Li^2];

    teta=atan((Y(i)-Y(i+1))/(X(i)-X(i+1)));

    Trans=[cos(teta) sin(teta)
           -sin(teta) cos(teta)];

    if i==1
        k1=0;
        node2=Trans*([X(i+1);Y(i+1)]-C_0);
        node3=Trans*([X(i+2);Y(i+2)]-C_0);
        k2=((node2(2)-node3(2))/(node2(1)-node3(1)))*0.5;

        bc=[0 k1 0 k2]';
        alfa=inv(A)*bc;

        Ylocal=alfa(1)+alfa(2)*Li*0.5+alfa(3)*(Li*0.5)^2+alfa(4)*(Li*0.5)^3;

        CoordLocal=[Li*0.5;Ylocal];

        NewCoord=inv(Trans)*CoordLocal+C_0;

        GlobalCoord(i,:)=NewCoord';
    end
end
```

```
if i==nel
    k2=0;
    node2=Trans*([[X(i);Y(i)]-C_0]);
    node3=Trans*([[X(i-1);Y(i-1)]-C_0]);
    k1=((node3(2)-node2(2))/(node3(1)-node2(1)))*0.5;

    bc=[0 k1 0 k2]';
    alfa=inv(A)*bc;

    Ylocal=alfa(1)+alfa(2)*Li*0.5+alfa(3)*(Li*0.5)^2+alfa(4)*(Li*0.5)^3;

    CoordLocal=[Li*0.5;Ylocal];

    NewCoord=inv(Trans)*CoordLocal+C_0;

    GlobalCoord(i,:)=NewCoord';
end

if i~=1 && i~=nel
    node1=Trans*([[X(i-1);Y(i-1)]-C_0])
    node2=Trans*([[X(i+1);Y(i+1)]-C_0]);
    node3=Trans*([[X(i+2);Y(i+2)]-C_0]);
    k2=((node2(2)-node3(2))/(node2(1)-node3(1)))*0.5;
    k1=((node1(2)-0)/(node1(1)-0))*0.5;

    bc=[0 k1 0 k2]';
    alfa=inv(A)*bc';

    Ylocal=alfa(1)+alfa(2)*Li*0.5+alfa(3)*(Li*0.5)^2+alfa(4)*(Li*0.5)^3;

    CoordLocal=[Li*0.5;Ylocal];

    NewCoord=inv(Trans)*CoordLocal+C_0;

    GlobalCoord(i,:)=NewCoord';
end
end
```

Appendix B

Material properties

Steel	
Density (kg/m ³)	7800
Elastic modulus (GPa)	210
Yield stress (MPa)	230
Etan (MPa)	500
Poissons ratio	0,3

Aluminium	
Density (kg/m ³)	3000
Elastic modulus (GPa)	68,3
Yield stress (MPa)	80
Etan (MPa)	250
Poissons ratio	0,3

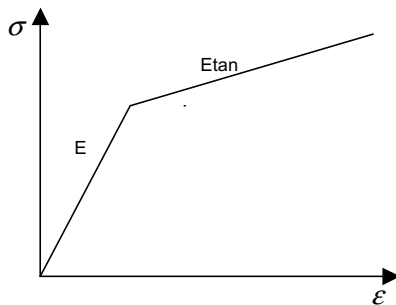


Figure B.1: Definition of Etan for the material properties